Comparative study of intracavity KTP-based Raman generation between Nd:YAP and Nd:YAG lasers operating on the $^4F_{3/2} \rightarrow {}^4I_{13/2}$ transition

Y. J. Huang,[1] Y. F. Chen,[1,2,*] W. D. Chen,[3] and G. Zhang[3]

[1]*Department of Electrophysics, National Chiao Tung University, Hsinchu 30010, Taiwan*
[2]*Department of Electronics Engineering, National Chiao Tung University, Hsinchu 30010, Taiwan*
[3]*Key Laboratory of Optoelectronic Materials Chemistry and Physics, Fujian Institute of Research on the Structure of Matter, Chinese Academy of Sciences, Fuzhou, Fujian, 350002, China*
[*]*yfchen@cc.nctu.edu.tw*

Abstract: Extending the spectral wavelengths of the diode-pumped Nd-doped lasers at 1.3 μm with the KTP crystal in the intracavity Raman configuration is reported for the first time to the best of our knowledge. A systematic comparison is performed to show that a better optical conversion efficiency for the Nd:YAP/KTP Raman laser could be achieved thanks to the higher peak power and linearly polarized radiation at 1341 nm, whereas up to four Stokes emission lines are generated from the Nd:YAG/KTP Raman laser as a result of the fundamental dual-color operation at 1319 and 1338 nm. The maximum Stokes output power of the developed Nd:YAP/KTP Raman laser reaches 1.04 W under an incident pump power of 16 W and a pulse repetition rate of 10 kHz, corresponding to the diode-to-Stokes conversion efficiency as high as 6.5%. The largest pulse energy and highest peak power are evaluated to be up to 104 μJ and 34.7 kW, respectively.

OCIS codes: (140.3550) Lasers, Raman; (140.3540) Lasers, Q-switched; (140.3580) Lasers, solid-state; (140.3480) Lasers, diode-pumped; (140.3530) Lasers, neodymium.

References and links

1. M. J. Weber, M. Bass, K. Andringa, R. R. Monchamp, and E. Comperchio, "Czochralski growth and properties of $YAlO_3$ laser crystals," Appl. Phys. Lett. **15**(10), 342–345 (1969).
2. M. J. Weber and T. E. Varitimos, "Optical spectra and intensities of Nd^{3+} in $YAlO_3$," J. Appl. Phys. **42**(12), 4996–5005 (1971).
3. A. A. Kaminskii, S. E. Sarkisov, I. V. Mochalov, L. K. Aminov, and A. O. Ivanov, "Anisotropy of spectroscopic characteristics in the biaxial $YAlO_3$-Nd^{3+} laser crystals," Phys. Stat. Solidi **51**(2), 509–520 (1979).
4. F. Hanson and P. Poirier, "Multiple-wavelength operation of a diode-pumped Nd:$YAlO_3$ laser," J. Opt. Soc. Am. B **12**(7), 1311–1315 (1995).
5. R. F. Wu, K. S. Lai, H. Wong, W. J. Xie, Y. Lim, and E. Lau, "Multiwatt mid-IR output from a Nd:YALO laser pumped intracavity KTA OPO," Opt. Express **8**(13), 694–698 (2001).
6. H. Y. Zhu, Y. M. Duan, G. Zhang, C. H. Huang, Y. Wei, W. D. Chen, H. Y. Wang, and G. Qiu, "High-power LD end-pumped intra-cavity Nd:$YAlO_3$/$KTiOAsO_4$ optical parametric oscillator emitting at 1562 nm," Laser Phys. Lett. **7**(10), 703–706 (2010).
7. Y. Lü, P. Zhai, J. Xia, X. Fu, and S. Li, "Simultaneous orthogonal polarized dual-wavelength continuous-wave laser operation at 1079.5 nm and 1064.5 nm in Nd:$YAlO_3$ and their sum-frequency mixing," J. Opt. Soc. Am. B **29**(9), 2352–2356 (2012).
8. H. Y. Zhu, Y. M. Duan, H. Y. Wang, Z. H. Shao, Y. J. Zhang, G. Zhang, J. Zhang, and D. Y. Tang, "Compact Nd:$YAlO_3$/$RbTiOPO_4$ based intra-cavity optical parametric oscillator emit at 1.65 and 3.13 μm," IEEE J. Sel. Top. Quantum Electron. **21**(1), 1600105 (2015).
9. Y. F. Chen, T. M. Huang, C. L. Wang, and L. J. Lee, "Compact and efficient 3.2-W diode-pumped Nd:YVO_4/KTP green laser," Appl. Opt. **37**(24), 5727–5730 (1998).
10. S. Bai and J. Dong, "GTR-KTP enhanced stable intracavity frequency doubled Cr,Nd:YAG self-Q-switched green laser," Laser Phys. **25**(2), 025002 (2015).
11. Y. F. Chen, Y. S. Chen, and S. W. Tsai, "Diode-pumped Q-switched laser with intracavity sum frequency mixing in periodically poled KTP," Appl. Phys. B **79**(2), 207–210 (2004).

#235322 - $15.00 USD Received 2 Mar 2015; revised 9 Apr 2015; accepted 10 Apr 2015; published 14 Apr 2015

12. J. Y. Huang, W. Z. Zhuang, Y. P. Huang, Y. J. Huang, K. W. Su, and Y. F. Chen, "Improvement of stability and efficiency in diode-pumped passively Q-switched intracavity optical parametric oscillator with a monolithic cavity," Laser Phys. Lett. **9**(7), 485–490 (2012).
13. Q. Cui, X. Shu, X. Le, and X. Zhang, "70-W average-power doubly resonant optical parametric oscillator at 2 μm with single KTP," Appl. Phys. B **117**(2), 639–643 (2014).
14. G. A. Massey, T. M. Loehr, L. J. Willis, and J. C. Johnson, "Raman and electrooptic properties of potaśsium titanate phosphate," Appl. Opt. **19**(24), 4136–4137 (1980).
15. Y. B. Band, J. R. Ackerhalt, J. S. Krasinski, and D. F. Heller, "Intracavity Raman lasers," IEEE J. Quantum Electron. **25**(2), 208–213 (1989).
16. H. M. Pask, "The design and operation of solid-state Raman lasers," Prog. Quantum Electron. **27**(1), 3–56 (2003).
17. P. Cerný, H. Jelínková, P. G. Zverev, and T. T. Basiev, "Solid state lasers with Raman frequency conversion," Prog. Quantum Electron. **28**(2), 113–143 (2004).
18. J. A. Piper and H. M. Pask, "Crystalline Raman lasers," IEEE J. Sel. Top. Quantum Electron. **13**(3), 692–704 (2007).
19. G. H. Watson, "Polarized Raman spectra of $KTiOAsO_4$ and isomorphic nonlinear-optical crystals," J. Raman Spectrosc. **22**(11), 705–713 (1991).
20. C. S. Tu, A. R. Guo, R. Tao, R. S. Katiyar, R. Guo, and A. S. Bhalla, "Temperature dependent Raman scattering in $KTiOPO_4$ and $KTiOAsO_4$ single crystals," J. Appl. Phys. **79**(6), 3235–3240 (1996).
21. Y. F. Chen, "Stimulated Raman scattering in a potassium titanyl phosphate crystal: simultaneous self-sum frequency mixing and self-frequency doubling," Opt. Lett. **30**(4), 400–402 (2005).
22. S. Pearce, C. L. M. Ireland, and P. E. Dyer, "Solid-state Raman laser generating <1 ns, multi-kilohertz pulses at 1096 nm," Opt. Commun. **260**(2), 680–686 (2006).
23. Y. T. Chang, Y. P. Huang, K. W. Su, and Y. F. Chen, "Diode-pumped multi-frequency Q-switched laser with intracavity cascade Raman emission," Opt. Express **16**(11), 8286–8291 (2008).
24. Z. Liu, Q. Wang, X. Zhang, Z. Liu, J. Chang, H. Wang, S. Zhang, S. Fan, W. Sun, G. Jin, X. Tao, S. Zhang, and H. Zhang, "A $KTiOAsO_4$ Raman laser," Appl. Phys. B **94**(4), 585–588 (2009).
25. Z. J. Liu, Q. P. Wang, X. Y. Zhang, S. S. Zhang, J. Chang, H. Wang, S. Z. Fan, W. J. Sun, X. T. Tao, S. J. Zhang, and H. J. Zhang, "1120 nm second-Stokes generation in $KTiOAsO_4$," Laser Phys. Lett. **6**(2), 121–124 (2009).
26. H. T. Huang, J. L. He, and Y. Wang, "Second Stokes 1129 nm generation in gray-trace resistance KTP intracavity driven by a diode-pumped Q-switched Nd:YVO_4 laser," Appl. Phys. B **102**(4), 873–878 (2011).
27. H. Zhu, Z. Shao, H. Wang, Y. Duan, J. Zhang, D. Tang, and A. A. Kaminskii, "Multi-order Stokes output based on intra-cavity $KTiOAsO_4$ Raman crystal," Opt. Express **22**(16), 19662–19667 (2014).
28. G. Kh. Kitaeva, "Terahertz generation by means of optical lasers," Laser Phys. Lett. **5**(8), 559–576 (2008).
29. P. Zhao, S. Ragam, Y. J. Ding, and I. B. Zotova, "Power scalability and frequency agility of compact terahertz source based on frequency mixing from solid-state lasers," Appl. Phys. Lett. **98**(13), 131106 (2011).
30. W. Wang, Z. Cong, X. Chen, X. Zhang, Z. Qin, G. Tang, N. Li, C. Wang, and Q. Lu, "Terahertz parametric oscillator based on $KTiOPO_4$ crystal," Opt. Lett. **39**(13), 3706–3709 (2014).
31. H. Li, R. K. Hanson, and J. B. Jeffries, "Diode laser-induced infrared fluorescence of water vapour," Meas. Sci. Technol. **15**(7), 1285–1290 (2004).
32. A. D. Griffiths and A. F. P. Houwing, "Diode laser absorption spectroscopy of water vapor in a scramjet combustor," Appl. Opt. **44**(31), 6653–6659 (2005).
33. H. Li, A. Farooq, J. B. Jeffries, and R. K. Hanson, "Near-infrared diode laser absorption sensor for rapid measurements of temperature and water vapor in a shock tube," Appl. Phys. B **89**(2–3), 407–416 (2007).
34. E. Gregor, D. E. Nieuwsma, and R. D. Stultz, "20 Hz eyesafe laser rangefinder for air defense," Proc. SPIE **1207**, 124–135 (1990).
35. L. R. Marshall, J. Kasinski, and R. L. Burnham, "Diode-pumped eye-safe laser source exceeding 1% efficiency," Opt. Lett. **16**(21), 1680–1682 (1991).
36. H. Y. Zhu, G. Zhang, C. H. Huang, Y. Wei, L. X. Huang, A. H. Li, and Z. Q. Chen, "1318.8 nm/1338.2 nm simultaneous dual-wavelength Q-switched Nd:YAG laser," Appl. Phys. B **90**(3–4), 451–454 (2008).
37. H. Liu, M. Gong, X. Wushouer, and S. Gao, "Compact corner-pumped Nd:YAG/YAG composite slab 1319 nm/1338 nm laser," Laser Phys. Lett. **7**(2), 124–129 (2010).
38. L. Guo, R. Lan, H. Liu, H. Yu, H. Zhang, J. Wang, D. Hu, S. Zhuang, L. Chen, Y. Zhao, X. Xu, and Z. Wang, "1319 nm and 1338 nm dual-wavelength operation of LD end-pumped Nd:YAG ceramic laser," Opt. Express **18**(9), 9098–9106 (2010).
39. Y. Duan, H. Zhu, C. Xu, H. Yang, D. Luo, H. Lin, J. Zhang, and D. Tang, "Comparison of the 1319 and 1338 nm dual-wavelength emission of neodymium-doped yttrium aluminum garnet ceramic and crystal lasers," Appl. Phys. Express **6**(1), 012701 (2013).
40. W. Chen, Y. Inagawa, T. Omatsu, M. Tateda, N. Takeuchi, and Y. Usuki, "Diode-pumped, self-stimulating, passively Q-switched Nd^{3+}:$PbWO_4$ Raman laser," Opt. Commun. **194**(4–6), 401–407 (2001).
41. A. A. Demidovich, P. A. Apanasevich, L. E. Batay, A. S. Grabtchikov, A. N. Kuzmin, V. A. Lisinetskii, V. A. Orlovich, O. V. Kuzmin, V. L. Hait, W. Kiefer, and M. B. Danailov, "Sub-nanosecond microchip laser with intracavity Raman conversion," Appl. Phys. B **76**(5), 509–514 (2003).
42. R. Frey, A. de Martino, and F. Pradère, "High-efficiency pulse compression with intracavity Raman oscillators," Opt. Lett. **8**(8), 437–439 (1983).

#235322 - $15.00 USD Received 2 Mar 2015; revised 9 Apr 2015; accepted 10 Apr 2015; published 14 Apr 2015

43. J. T. Murray, W. L. Austin, and R. C. Powell, "Intracavity Raman conversion and Raman beam cleanup," Opt. Mater. **11**(4), 353–371 (1999).

1. Introduction

The output characteristics of solid-state lasers are mainly determined by the gain medium. To date, the Nd:YAG crystal, due to its excellent mechanical and optical properties, is widely studied in developing various kinds of laser architectures and popularly utilized in commercial products. From a review of previous literatures, it was pointed out that the Nd:YAP crystal, also known as Nd:YAlO or Nd:$YAlO_3$, is a suitable candidate for replacing the Nd:YAG crystal while keeping some similar physical properties such as hardness and thermal conductivity. Although these two host materials are both derived from the Y_2O_3-Al_2O_3 system [1–3], the different composition ratios lead the crystalline host to be orthorhombic in the Nd:YAP crystal rather than cubic in the Nd:YAG crystal. Therefore, a more efficient nonlinear wavelength conversion could usually be readily achieved with the Nd:YAP laser thanks to the linearly polarized emission as a result of the natural crystal birefringence [4–8].

The potassium titanyl phosphate (KTP) crystal is a well-known nonlinear crystal for producing coherent radiations covering a large portion of the spectral range through second harmonic generation [9,10], sum and difference frequency generation [7,11], and optical parametric oscillation [12,13]. Besides the second-order nonlinear response, the early research of the spontaneous Raman spectrum [14] indicated the feasibility of the KTP crystal to be a practical frequency converter via stimulated Raman scattering (SRS), an attractive method of wavelength conversion based on the third-order nonlinearity [15–18]. The isomorphs of the KTP crystal, including the potassium titanyl arsenate (KTA) and rubidium titanyl phosphate (RTP) materials, were also identified as efficient Raman-active media [19,20], and over the past few years, the intracavity generation of coherent Stokes waves driven by diode-pumped Nd-doped lasers at 1.06 μm has been extensively demonstrated based on the X(ZZ)X configuration [21–27]. In comparison with other crystalline Raman materials such as vanadates and tungstates, the relatively small frequency shifts of the KTP crystal and its isomorphs allow for easily acquiring multiple Stokes emission lines through cascaded SRS process, which are desirable for producing coherent terahertz radiation by different frequency generation [28–30]. Even so, to the best of our knowledge, the KTP-based SRS process has not been realized to extend the spectral wavelengths of the Nd-doped lasers operating on the $^4F_{3/2} \rightarrow {}^4I_{13/2}$ transition.

In this work, we originally demonstrate an intracavity KTP-based Raman radiation with a frequency shift of 267 cm^{-1} in a compact diode-end-pumped actively Q-switched Nd:YAP laser at 1341 nm for the first time. Under an incident pump power of 16 W and a pulse repetition rate of 10 kHz, the total Raman output power of 1.04 W, including the first and second Stokes components of 0.46 W at 1391 nm and 0.58 W at 1445 nm, is efficiently generated with a pulse duration as short as 3 ns, corresponding to the diode-to-Stokes conversion efficiency of up to 6.5%. The largest pulse energy and highest peak power are evaluated to be 104 μJ and 34.7 kW, respectively. We also prepare a Nd:YAG crystal to make a systematic comparison under a similar operating condition. It is experimentally found that although lower output power is obtained from the Nd:YAG/KTP Raman laser, up to four Stokes emission lines could be produced thanks to the dual-wavelength operation of the fundamental wave at 1319 and 1338 nm. The first and second Stokes spectral wavelengths generated in our developed KTP-based Raman oscillators can find their usefulness in the moisture and water-vapor detections [31–33] as well as laser radar, range finder, telemetry, and other remote-sensing applications [34,35].

2. Experimental setup

Figure 1 schematically depicts the experimental arrangement of intracavity Raman oscillator based on the KTP crystal pumped by diode-end-pumped actively Q-switched Nd-doped lasers at 1.3 μm, where a shared configuration for the fundamental and Stokes wavelengths was

#235322 - $15.00 USD Received 2 Mar 2015; revised 9 Apr 2015; accepted 10 Apr 2015; published 14 Apr 2015

utilized. The pump source was a fiber-coupled laser diode at 808 nm with a core diameter of 800 μm and a numerical aperture of 0.14. A pair of plano-convex coupling lenses with focal lengths of 25.4 mm was utilized to reimage the pump beam into the laser crystal with a spot radius of 400 μm. The input mirror was a plane mirror that is coated for anti-reflection (AR, R < 0.2%) at 808 nm on the entrance surface, and for high reflection (HR, R > 99.8%) in the range of 1300-1500 nm as well as for high transmission (HT, T > 90%) at 808 nm on the other surface. The Nd:YAP and Nd:YAG crystals were employed for conducting a systematic comparison at the fundamental and Stokes wavelengths. The Nd:YAP crystal with the dimension of 3 × 3 × 10 mm^3 was with the doping concentration of 1%, whereas the Nd:YAG crystal with the diameter of 4 mm and the length of 10 mm was with the doping concentration of 0.8%. The KTP crystal with the size of 4 × 4 × 20 mm^3 was x-cut along $\theta = 90°$ and $\phi = 0°$ to realize the X(ZZ)X configuration in the SRS process. Both sides of the Nd:YAP, Nd:YAG, and KTP crystals were AR coated in the range of 1300-1500 nm. These crystals were also wrapped with indium foil and mounted in water-cooled copper holders at a temperature of 18°C. A 20-mm-long acousto-optical Q-switch (Gooch & Housego) had AR coating at lasing wavelengths on both sides, and it was driven at RF frequency and power of 41 MHz and 25 W. A plane mirror with HR coating at the fundamental wavelength was used as the Raman output coupler. Its reflectivity gradually decreases with the increase of the wavelength from 1350 to 1480 nm. The values of reflectivities for fundamental wavelengths and individual Stokes emission lines that would be generated in the experiment are as follows: R = 99.5% at 1319, 1338, and 1341 nm, R = 99.0% at 1368 nm, R = 98.5% at 1389 and 1391 nm, R = 91.31% at 1420 nm, R = 29.1% at 1442 nm, and R = 25.8% at 1445 nm. All optical components were placed as close as possible to have a cavity length of 77 mm.

The spectral information on the laser output was registered by an optical spectrum analyzer (Advantest, Q8381A) that employs a diffraction lattice monochromator for high-speed measurement of pulse light with a resolution of 0.1 nm. The pulse temporal behaviors were recorded by a digital oscilloscope (LeCroy, Wavepro 7100, 10 G samples/s, 1 GHz bandwidth) with a fast InGaAs photodiode.

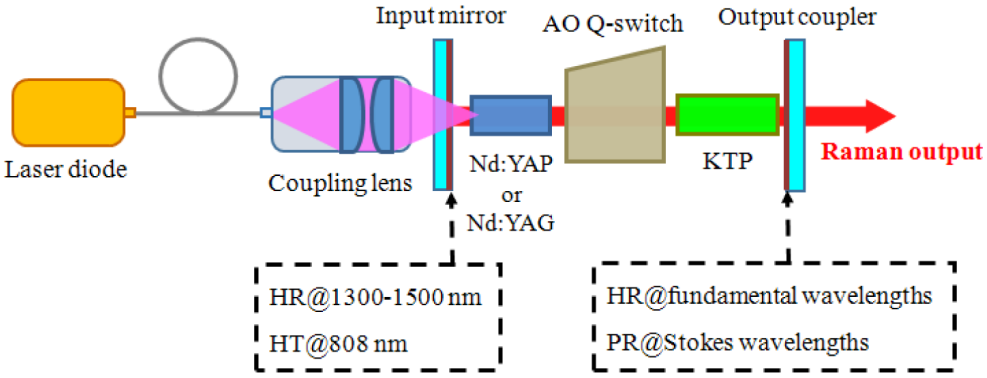

Fig. 1. Experimental setup of intracavity KTP-based Raman oscillator pumped by diode-end-pumped actively Q-switched Nd-doped lasers at 1.3 μm.

3. Comparative study between the Nd:YAP and Nd:YAG lasers operating on the $^4F_{3/2} \rightarrow {}^4I_{13/2}$ transition

First of all, the actively Q-switched performances at the fundamental wavelength for the Nd:YAP and Nd:YAG lasers were comparatively studied, where the aforementioned Raman output coupler was replaced by a plane output coupler with a reflectivity of 96% in the range of 1300-1350 nm. Figures 2(a)-2(d) illustrate the results of average output power, pulse energy, pulse duration, and peak power at 1.3 μm as a function of the pulse repetition rate. The average output power and pulse energy for both lasers are experimentally found to be

#235322 - $15.00 USD Received 2 Mar 2015; revised 9 Apr 2015; accepted 10 Apr 2015; published 14 Apr 2015

quite comparable, as exhibited in Figs. 2(a) and 2(b). On the one hand, the average output power increases from 1.16 to 1.99 W and the pulse energy decreases from 232 to 100 μJ when the pulse repetition rate changes from 5 to 20 kHz for the Nd:YAP laser. On the other hand, the average output power raises from 1.24 to 1.9 W and the pulse energy reduces from 248 to 95 μJ as the pulse repetition rate varies from 5 to 20 kHz for the Nd:YAG laser. In contrast, the pulse duration obtained from the Nd:YAP laser is observed to be generally shorter than that obtained from the Nd:YAG laser by an amount of 20-30 ns, depending on the pulse repetition rate, as shown in Fig. 2(c). Consequently, the Nd:YAP laser could emit Q-switched pulses with higher peak power as compared with the Nd:YAG laser, as displayed in Fig. 2(d), where the largest values for the Nd:YAP and Nd:YAG laser are 3.9 and 3.1 kW, respectively. Figures 2(e) and 2(f) describe the optical spectra for both cases with the insets showing the measured room-temperature fluorescent profiles. The central wavelength for the Nd:YAP laser locates at 1341.3 nm with the full width at half maximum of approximately 0.2 nm. For the Nd:YAG laser, it was experimentally found that the dual-wavelength operation is achieved due to the comparable stimulated emission cross sections at 1319 and 1338 nm [36–39], as can also be deduced from the inset in Fig. 2(f).

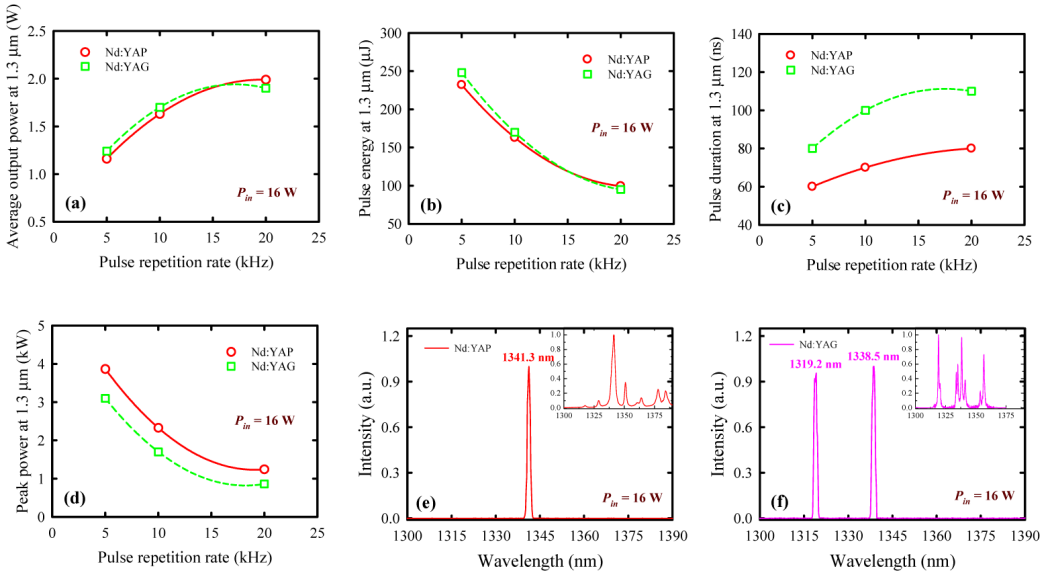

Fig. 2. (a) Average output power, (b) pulse energy, (c) pulse duration, and (d) peak power with respect to the pulse repetition rate under an incident pump power of 16 W for the Nd:YAP and Nd:YAG laser at 1.3 μm; Optical spectra for the (e) Nd:YAP and (f) Nd:YAG lasers with the insets showing the measured room-temperature fluorescent profiles.

4. Output characteristics of the intracavity KTP-based Raman generations

Then, the conversion efficiencies in the SRS process based on the KTP crystal were comparatively investigated with the Nd:YAP and Nd:YAG lasers operating on the $^4F_{3/2} \rightarrow {}^4I_{13/2}$ transition. The best results are achieved at a pulse repetition rate of 10 kHz. During the experiment, only the first and second Stokes emission lines were generated, and no higher-order Stokes wavelength was detected. The average output powers of the fundamental and individual Stokes components at a pulse repetition rate of 10 kHz are described in Fig. 3(a) for the Nd:YAP/KTP Raman laser. The fundamental output power is measured to be on the order of several tens of milliwatts in the whole operating range. The pump threshold for the first Stokes wave is about 5.1 W and its output power continuously increases with the pump power and then saturates at a level of around 0.46 W. When the pump power exceeds 6.9 W, the second Stokes radiation starts to emit and quickly grows up with the pump power, and

#235322 - $15.00 USD Received 2 Mar 2015; revised 9 Apr 2015; accepted 10 Apr 2015; published 14 Apr 2015

eventually becomes the dominant portion of the Raman output. At the maximum incident pump power of 16 W, the total Raman output power of 1.04 W, containing the first and second Stokes components of 0.46 and 0.58 W, is efficiently generated, corresponding to the diode-to-Stokes conversion efficiency of up to 6.5%. Alternatively, the conversion efficiency with respect to the output power available from the fundamental laser at 1341 nm reaches 63.8%. The Raman pulse energy is evaluated to be 104 μJ under a pulse repetition rate of 10 kHz. For the Nd:YAG/KTP Raman laser, similar behaviors for the fundamental and Stokes waves are obtained except that the pump thresholds for the first and second Stokes components are increased to be 6.2 and 8.9 W, as illustrated in Fig. 3(b). At the maximum incident pump power of 16 W, lower total Raman output power of 0.47 W is obtained, including the first and second Stokes components of 0.09 and 0.38 W, respectively. The conversion efficiencies with respect to the input diode power and the output power obtainable from the fundamental laser at 1.3 μm are 2.9 and 27.6%, respectively. The Raman pulse energy is estimated to be 47 μJ under a pulse repetition rate of 10 kHz. The lower peak power and randomly polarized emission offered by the fundamental Q-switched Nd:YAG laser might be the reason why the considerably lower conversion efficiency in the SRS process is acquired for the Nd:YAG/KTP Raman laser.

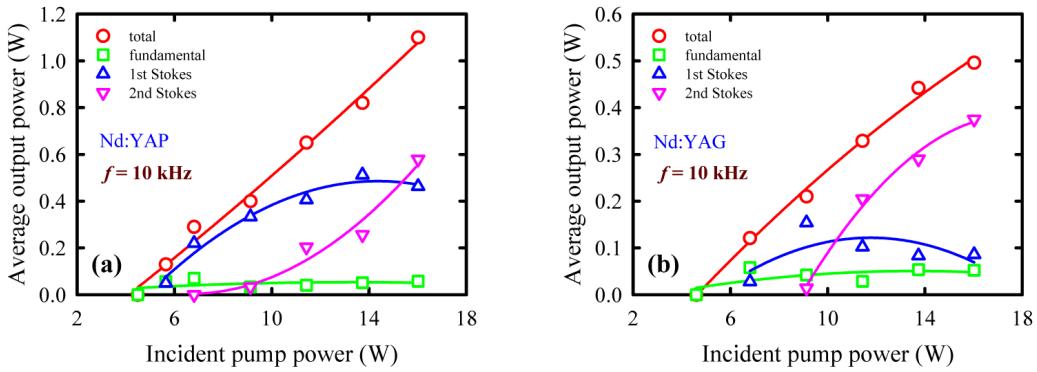

Fig. 3. Average output powers of the fundamental and individual Stokes components at a pulse repetition rate of 10 kHz for the (a) Nd:YAP/KTP and (b) Nd:YAG/KTP Raman lasers.

The behavior of the cascaded SRS process for the current KTP-based Raman laser could be understood more clearly with the help of a set of spatially independent coupled rate equations, which describe the temporal evolutions of the population inversion density n, the intracavity fundamental photon density ϕ_0, and the intracavity ith-order Stokes photon density ϕ_i [40,41]:

$$\frac{dn}{dt} = r_p - c\sigma n\phi_0 - \frac{n}{\tau} \tag{1}$$

$$\frac{d\phi_0}{dt} = \frac{\phi_0}{T_r}\left[2\sigma n l_g - 2gh\nu_0 c\phi_1 l_R\right] - \frac{\phi_0}{\tau_0} \tag{2}$$

$$\frac{d\phi_i}{dt} = \frac{\phi_i}{T_r}\left[2gh\nu_{i-1} c\phi_{i-1} l_R - 2gh\nu_i c\phi_{i+1} l_R\right] - \frac{\phi_i}{\tau_i}, \text{ for } i = 1...N-1 \tag{3}$$

$$\frac{d\phi_i}{dt} = \frac{\phi_i}{T_r}\left[2gh\nu_{i-1} c\phi_{i-1} l_R\right] - \frac{\phi_i}{\tau_i}, \text{ for } i = N \tag{4}$$

where r_p is the rate of the pump density, c is the speed of light, σ and τ are the stimulated emission cross section and the upper-state lifetime of the gain medium, T_r is the photon

#235322 - $15.00 USD Received 2 Mar 2015; revised 9 Apr 2015; accepted 10 Apr 2015; published 14 Apr 2015

round-trip time in the resonator, l_g is the length of the gain medium, g is the Raman gain parameter, h is the Planck constant, τ_0 is the photon lifetime at the fundamental light frequency v_0, l_R is the length of the Raman-active material, τ_i is the photon lifetime of the ith-order Stokes wave at the light frequency v_i, and N represents the highest order that the Raman laser could be generated. For the specific ith-order Stokes pulse to build up, the first derivative of ϕ_i with respect to time should be greater than zero, which means the following criterion should be satisfied:

$$\phi_{i-1} = \frac{T_r}{\tau_i} \frac{1}{2ghv_{i-1}cl_R} \tag{5}$$

It is apparent that when the photon number of lower (i-1)th-order Stokes wave reaches a certain threshold value given by Eq. (5), it can act as the pump source to produce the next higher ith-order Stokes radiation through the SRS conversion. This process could be repeatedly performed until the highest Nth-order Stokes beam generates.

The optical spectra at incident pump powers of 5.5, 6.8, 11.4, and 16 W are exhibited in Figs. 4(a)-4(d) for the Nd:YAP/KTP Raman laser. The evolution of the optical spectra with respect to the incident pump power is consistent with the behaviors of output powers for individual spectral components recorded in Fig. 3(a). As shown in Fig. 4(d), the central wavelengths of the first and second Stokes radiations are measured to be 1391.4 and 1444.9 nm, respectively. The frequency shifts between the Stokes emission lines and the fundamental wavelength at 1341 nm agree very well with the asymmetric bending mode of a distorted TiO_6 octahedron (267 cm^{-1}). For the Nd:YAG/KTP Raman oscillator, Figs. 4(a')-4(d') describe the optical spectra at incident pump powers of 5.5, 6.8, 11.4, and 16 W. Intriguingly, it is experimentally found that up to four Stokes spectral lines could be derived from the dual-wavelength Nd:YAG laser at 1.3 μm. Through the cascaded SRS process, the Stokes waves at 1367.9 and 1420.5 nm are created by the fundamental light at 1319.2 nm, while the Stokes radiations at 1388.7 and 1441.7 nm are originated from the fundamental light at 1338.5 nm. These results imply that the cascaded SRS conversion from the multi-wavelength laser might be a promising approach to emit a wealth of spectral lines with small wavelength separations. During the experiment, weak red lights were also observed for both Nd:YAP/KTP and Nd:YAG/KTP Raman lasers as a result of second and sum frequency generations for the fundamental and Stokes waves in the KTP crystal, as shown in Figs. 4(e) and 4(e'), respectively.

#235322 - $15.00 USD Received 2 Mar 2015; revised 9 Apr 2015; accepted 10 Apr 2015; published 14 Apr 2015

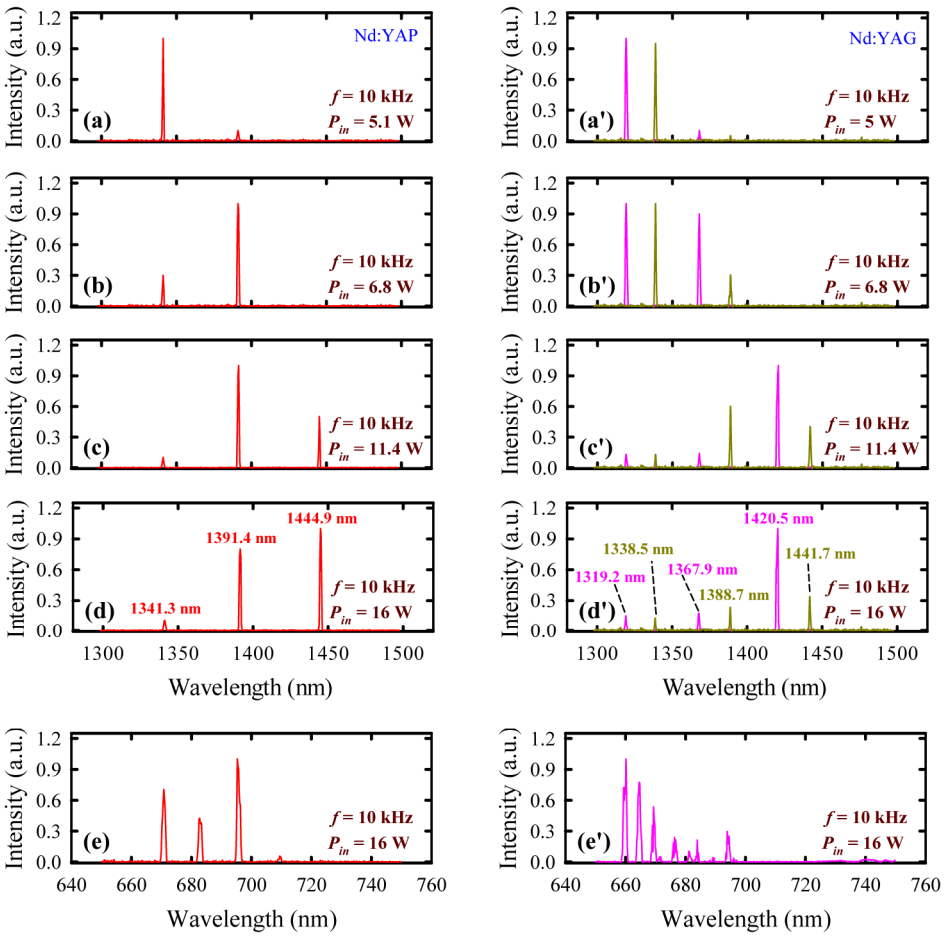

Fig. 4. Optical spectra in the near infrared region at incident pump powers of (a) 5.5 W, (b) 6.8 W, (c) 11.4 W, and (d) 16 W, as well as the (e) optical spectrum in the visible region, for the Nd:YAP/KTP Raman laser under a pulse repetition rate of 10 kHz; (a')-(e') being the corresponding cases for the Nd:YAG/KTP Raman laser.

Typical temporal behaviors of the residual fundamental and Raman output pulses at an incident pump power of 16 W and a pulse repetition rate of 10 kHz are illustrated in Fig. 5. The pulse-to-pulse amplitude stabilities are experimentally found to be better than ± 10% for both Nd:YAP/KTP and Nd:YAG/KTP Raman pulses, as depicted in Figs. 5(a) and 5(c). It can be seen that the depletion of the falling edge of the fundamental light is accompanied with the quick build-up of the Stokes wave. Furthermore, the nonlinear frequency conversion of the SRS process leads to the significant pulse shortening for the Raman laser as compared with the fundamental light [42]. For the Nd:YAP/KTP Raman laser, the shortest Stokes pulse duration illustrated in Fig. 5(b) is as narrow as 3 ns, corresponding to the peak power as high as 34.7 kW. For the Nd:YAG/KTP Raman laser, the shortest Stokes pulse duration described in Fig. 5(d) is 5 ns, corresponding to the peak power of 10 kW. Finally, because of the beam clean-up effect of the SRS process [43], the beam qualities for the Stokes radiation were generally found to be better than those of the fundamental light. With a knife-edge method, the beam quality factors of the Raman lasers are measured to both be M^2 <1.5 for orthogonal directions.

#235322 - $15.00 USD Received 2 Mar 2015; revised 9 Apr 2015; accepted 10 Apr 2015; published 14 Apr 2015

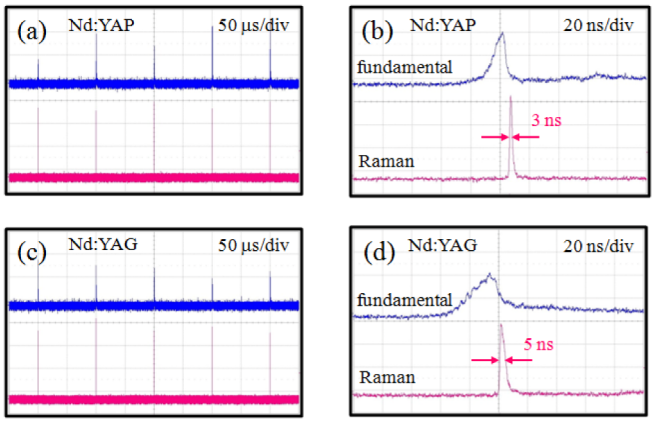

Fig. 5. Oscilloscope traces at an incident pump powers of 16 W and a pulse repetition rate of 10 kHz for the Nd:YAP/KTP Raman laser with the time span of (a) 500 μs and (b) 200 ns; and those for the Nd:YAG/KTP Raman laser with the time span of (c) 500 μs and (d) 200 ns.

5. Conclusion

In summary, the KTP crystal has been successfully employed as an intracavity Raman-active medium for extending the spectral ranges of the diode-pumped Nd:YAP and Nd:YAG lasers operating on the $^4F_{3/2} \rightarrow {}^4I_{13/2}$ transition with the frequency shift of 267 cm^{-1} for the first time. Experimental results have clearly shown that although up to four Stokes emission lines could be generated from the Nd:YAG/KTP Raman laser due to the fundamental dual-wavelength operation at 1319 and 1338 nm, the higher peak power and linearly polarized emission result in a better SRS conversion efficiency for the Nd:YAP/KTP Raman laser. Under an incident pump power of 16 W and a pulse repetition rate of 10 kHz, the developed Nd:YAP/KTP Raman laser efficiently generated a total output power of 1.04 W with a pulse duration down to 3 ns, where the first and second Stokes output powers were 0.46 and 0.58 W. The corresponding diode-to-Stokes conversion efficiency was up to 6.5%. The largest pulse energy and highest peak power of the developed Raman laser were evaluated to be up to 104 μJ and 34.7 kW, respectively.

Acknowledgments

The authors thank the Ministry of Science and Technology for their financial support of this research under Contract No. MOST 103-2112-M-009-016-MY3, and this work had also been supported by the National Natural Science Foundation of China under Grant No. 11404332.

#235322 - $15.00 USD Received 2 Mar 2015; revised 9 Apr 2015; accepted 10 Apr 2015; published 14 Apr 2015